17th World Conference on Earthquake Engineering, 17WCEE
Sendai, Japan - September 13th to 18th 2020

THE 2019 TOKYO METROPOLITAN RESILIENCE PROJECT E-DEFENSE TEST OF A 3-STORY DISASTER MANAGEMENT CENTER

TZ. Yeow[1], K. Kusunoki[2], I. Nakamura[3], Y. Hibino[4], T. Ohkubo[5], T. Seike[6], S. Yagi[7], T. Mukai[8], P. Calvi[9], M. Moustafa[10], S. Fukai[11]

[1] *Project Researcher, Earthquake Research Institute, University of Tokyo, trevoryeow@eri.u-tokyo.ac.jp*
[2] *Professor, Earthquake Research Institute, University of Tokyo, kusunoki@eri.u-tokyo.ac.jp*
[3] *Chief Researcher, National Research Institute for Earth Science and Disaster Resilience, izumi@bosai.go.jp*
[4] *Associate Professor, Graduate School of Engineering, Hiroshima University, hibino@hiroshima-u.ac.jp*
[5] *Professor, Graduate School of Engineering, Hiroshima University, ohkubotk@hiroshima-u.ac.jp*
[6] *Associate Professor, Graduate School of Frontier Sciences, University of Tokyo, seike@edu.k.u-tokyo.ac.jp*
[7] *Masters Candidate, Graduate School of Frontier Sciences, University of Tokyo, aboyleo872@gmail.com*
[8] *Senior Researcher, Building Research Institute, t_mukai@kenken.go.jp*
[9] *Assistant Professor, Civil and Environmental Engineering, University of Washington, pmc85@uw.edu*
[10] *Assistant Professor, Department of Civil and Environmental Engineering, University of Nevada, Reno, mmoustafa@unr.edu*
[11] *Professional Engineer, Structural Engineering Division, Nikken Sekkei Ltd, fukai@nikken.jp*

Abstract

Several buildings with post-disaster functions, such as city halls or emergency shelters, had been severely damaged in recent earthquakes in Japan; hindering their intended usage after a major seismic event. Furthermore, resource-intensive post-earthquake damage evaluation of buildings conducted after major seismic events often result in occupants being displaced from potentially safe buildings or delays in identifying dangerous buildings. There is also the potential for significant damage to be hidden and missed during damage evaluations. Based on this, there is a need to improve the resiliency of buildings with post-disaster functions and develop structural health monitoring techniques to rapidly and reliably assess the safety of buildings following major seismic shaking.

To address this need, an E-Defense test of a 3-story reinforced concrete disaster management center fitted with non-structural components and structural health monitoring instruments was performed under the Tokyo Metropolitan Resilience Project (subproject C). The specimen had hanging/standing/wing walls casted to be monolithic with frame elements. Gaps were present at the end of walls attached to the beams on the 2nd and 3rd floors, while gaps at the end of walls on the roof and at the 1F column bases were filled with concrete. These details allowed plastic hinges to form at intended locations and avoided bar buckling failure, while filling the gap with concrete allowed the wall to act only in compression. Non-structural elements attached to the building were ceilings, windows, exterior tiles and piping on the roof. Instrumentations and equipment installed in the building or used to evaluate damage included accelerometers, potentiometers, laser transducers, cameras, laser scanners, strain gauges and optical fibers; among others. In addition to the testing, a blind prediction competition was held to evaluate the accuracy and applicability of numerical modelling approaches and assumptions for buildings of this type.

An organized session based solely on this experimental study will be held at the 17th World Conference on Earthquake Engineering and will cover all aspects of the test. This paper serves as a companion piece for the organized session, and provides details on key aspects of the test, such as project background information, specimen details, test objectives, and input excitations. It will also cover preliminary damage observations and damage evaluations, showcase the application of the structural health monitoring approaches, and provide an overview of the blind prediction competition. Overall, it was found that the building mostly satisfied its performance objectives, and that the structural health monitoring methods adopted provided a rapid and reliable method to assess building damage and response.

Keywords: reinforced concrete, shake-table test, non-structural element, structural health monitoring, damage estimation,

1. Introduction

An E-Defense shake-table test of a 3-story reinforced concrete (RC) disaster management center was performed in December 2019 as part of the Tokyo Metropolitan Resilience Project Subproject C [1]. An organized session for this study will be held at the 17th World Conference on Earthquake Engineering, and will cover various topics ranging from project background, test details, performance assessment, structural health monitoring, and results from a blind prediction competition. This paper serves as a complementary source of information for interested conference participants who wish to learn more about the project.

2. Project Background and Objectives

The Tokyo Metropolitan area, while a major global economic center and home to over 35 million people, is a seismically active region. To reduce socioeconomic impacts from major seismic events, the "Tokyo Metropolitan Resilience Project" was initiated in 2017 and consisted of three subgroups; (i) social-sciences (subproject A), (ii) natural sciences (subproject B), and (iii) engineering (subproject C).

One objective of subproject C was the development of rapid damage assessment systems to avoid unnecessarily displacing people from safe buildings or to quickly identify dangerous buildings. Furthermore, such systems may be able to detect hidden damage, which was one of many reasons for the CTV Building collapse in New Zealand [2]. Another objective was to evaluate the effectiveness of resilient structural and non-structural detailing for buildings with post-disaster functions due to poor performance of such buildings in recent events (e.g. city hall buildings [3] and school gymnasiums intended to be used as emergency shelters [4]). There are other objectives in subproject C which have been/will be addressed by other research studies.

A shake-table test of a disaster management building was performed at E-Defense to address the two objectives discussed. Following requirements for Japanese buildings with post-disaster functions [5], the specimen must have a base shear coefficient greater than 0.55 and remain elastic with interstory drifts less than 0.33% at design-level shaking. The building must also meet life-safety requirements at 1.5 times design-level shaking. To achieve these objectives, spandrel walls were casted to be monolithic with RC frame elements to provide additional stiffness and strength, with special detailing provided to ensure a favorable deformation mode. The building was fitted with non-structural elements, and various instrumentation and scanning equipment were used to assess the building's performance. The key objectives of this test were to:

i) Evaluate the effectiveness of the spandrel wall detailing to satisfy performance objectives for buildings with post-disaster functions.

ii) Evaluate the effectiveness of more resilience non-structural element detailing.

iii) Test the reliability and robustness of various structural health monitoring techniques.

3. Test Description

3.1 Structural details

The RC specimen layout and dimensions are shown in Fig. 1. Spandrel wall elements were casted to be monolithic with the frame elements with 50 mm wide gaps present at hanging/standing wall ends on 2F and 3F (Fig. 2a) to ensure that plastic hinges form at intended locations and to prevent bar buckling failure. Similar detail was used for RF hanging-walls and 1F wing-wall bases, except that the gaps were filled with concrete to allow the walls to act in compression. The gap detailing had been tested previously [6,7], while the concrete filled-gap detailing was new. Reinforcing details of frame elements parallel to the loading direction are shown in Fig. 3. Note that reinforcing in the RF hanging-wall and 1F wing-wall base was terminated 50 mm before its ends, and that the lower reinforcing layer for B1 beams was also terminated before intersecting G2 and G3 beams. Details for other frame elements are available from Fukai et al [8].

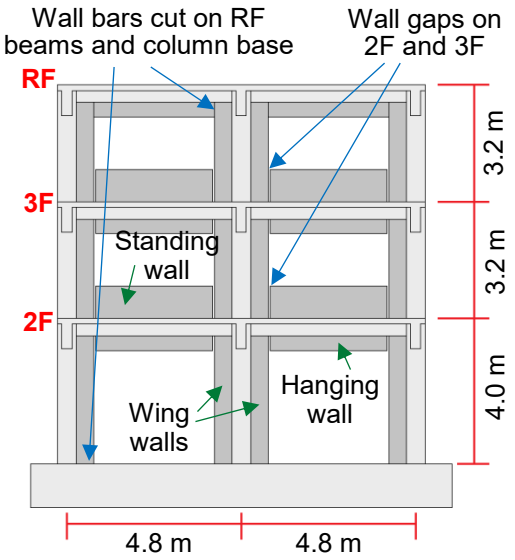

(a)

(b)

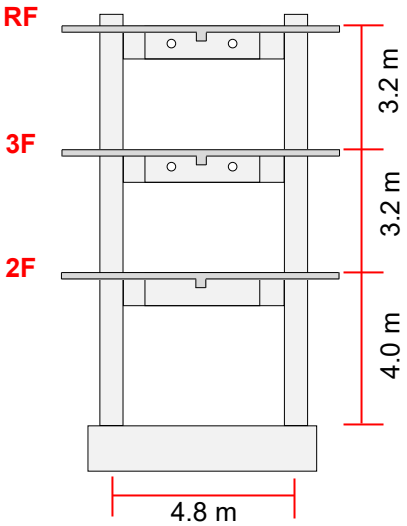

(c)

(d)

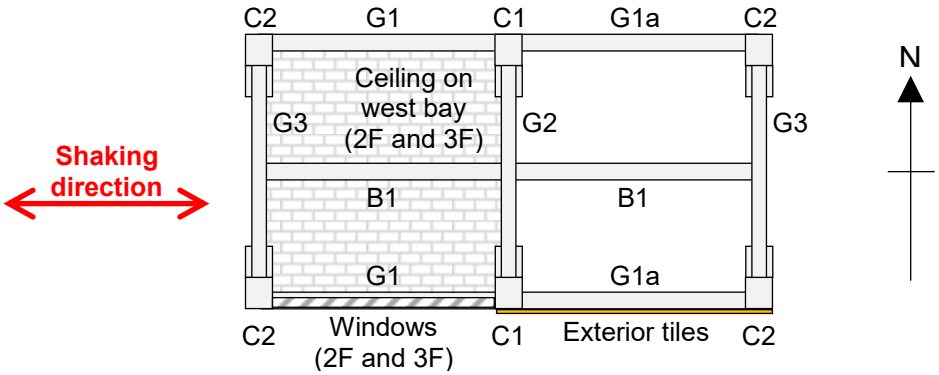

(e)

Fig. 1 – Specimen layout; (a) in-plane elevation dimensions, (b) in-plane elevation photo, (c) out-of-plane elevation dimensions, (d) out-of-plane elevation photo, and (e) location and ID of components

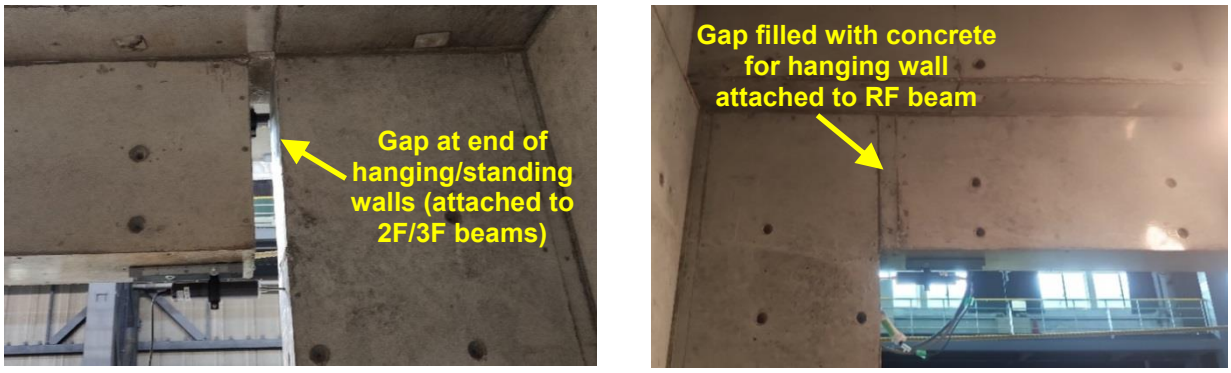

(a) (b)

Fig. 2 – Detailing at hanging/standing walls ends, (a) 50 mm gap at ends of hanging/standing walls attached to 2F/3F beams, (b) concrete filled gap on roof level beams (wall longitudinal reinforcing terminated)

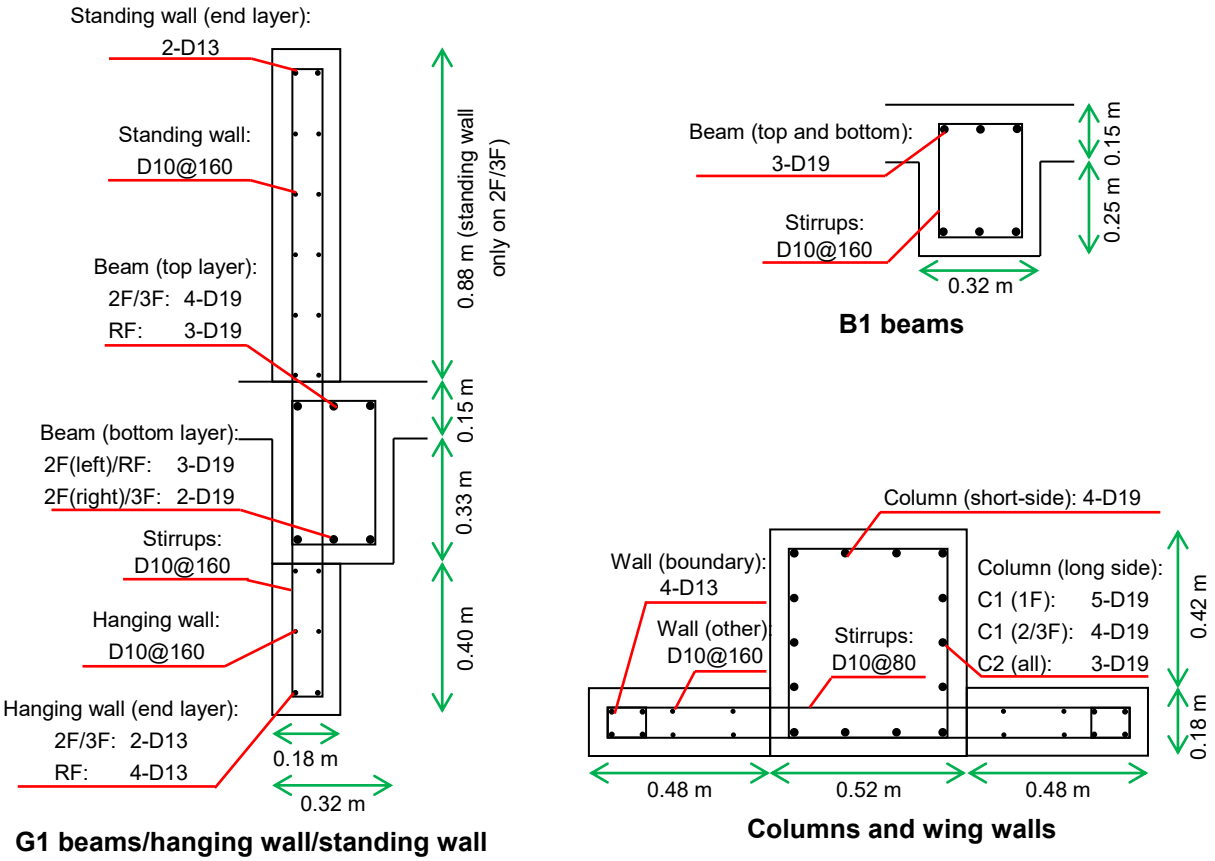

Fig. 3 – Cross section details

3.2 Non-structural details

Four types of non-structural components were attached to the building as follows:

i) Windows on south-west bay on 2F and 3F (Fig. 1e);

ii) Ceilings on west bay on 2F and 3F (Fig. 1e);

iii) Exterior tiles on south-east bay over entire height (Fig. 1e); and

iv) Piping on roof.

Two types of windows were installed in the building; fixed and sliding. The 2F fixed window used two panes of glass (Fig. 4a) while the 3F fixed window used a single pane (Fig. 4b). As the window sash used for both fixed windows were identical, the edge clearance is larger for the 2F fixed window and thus the drift capacity of the fixed window with two glass panes should be greater. The sliding windows were identical on both floors to observe the influence of drift demands on the seismic performance of sliding windows.

Two detailing variants were used for each non-structural component type; one being more seismically resilient than the other. With regards to ceilings, the one located on 2F (attached to 3F slabs) was fixed to the surrounding beams (Fig. 5a) without seismic bracing (Fig. 5b). The ceiling on 3F (attached to roof slab) had gaps around its edge (Fig. 5c) and was seismically braced (Fig. 5d). The latter ceiling was thought to be more seismically resistant and thus was installed where the acceleration demand was expected to be greater.

Two different materials were used to attach tiles to the south-east exterior bay; (a) mortar and (b) chemical adhesive. The mortar was applied over the western half of the bay, while the chemical adhesive was applied over the eastern half. The mortar layer was approximately 10 mm thicker, and thus a discontinuity of the tile surface could be observed as shown in Fig. 6. The chemical adhesive was more flexible than the mortar layer, and therefore the exterior tiles attached using the chemical adhesive were expected to remain attached to the frame at higher drift demands.

Two pipe systems in L-shape configurations were attached to the roof as shown in Fig. 7a. The pipes were weighed down using concrete supports instead of being bolted down as is common practice in Japan to avoid damaging roof weather proofing material. These supports had two or four-legs as shown in Fig. 7b, the latter of which was expected to be more stable and hence have lesser displacement.

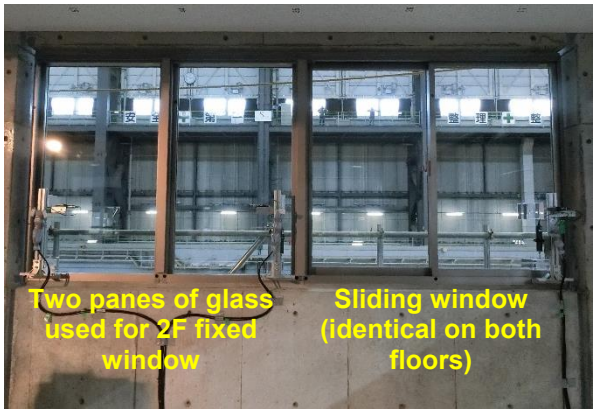

(a)

(b)

Fig. 4 – Window detailing; (a) two panes of glass used for 2F fixed window and (b) single pane of glass used for 3F fixed window

(a) (b) (c) (d)

Fig. 5 – Ceiling detailing; (a) no gaps for 2F ceiling, (b) no seismic braces for 2F ceiling, (c) edge gaps for 3F ceiling, and (d) seismic braces for 3F ceiling

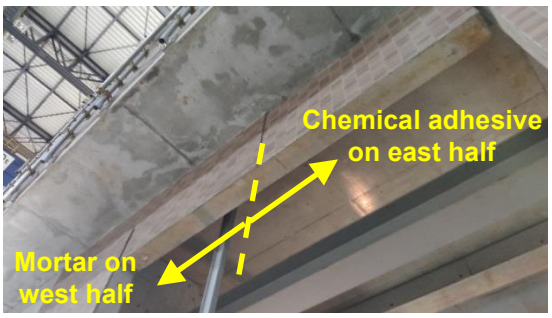

Fig. 6 – Tile detailing

(a) (b)

Fig. 7 – Pipe support detailing; (a) layout of piping and (b) difference in piping support

3.3 Instrumentation

Different types of accelerometers, such as those shown in Fig. 8a, were installed on all floors. This was to evaluate (i) the accuracy of cheaper sensors compared to more expensive variants and (ii) the global building performance following an approach proposed by Kusunoki et al. [9].

Laser transducers (Fig. 8b) were installed at three locations on each floor to measure interstory drift; one next to each exterior frame at the mid-width of the east-side bay and a third near the center of each floor. The transducer and the target were attached to steel H sections bolted to the bottom and top slab, respectively. The center location had two transducers in parallel to capture rotation effects.

Displacement potentiometers (Fig. 8c) were attached to the exterior of the northeast bay at column bases and joints between beams/hanging walls/standing walls and wing walls. These were also used on windows to capture window drift.

Other instrumentation and equipment installed in the building included video cameras, strain gauges, optical fibers, wires, and 3D scanners; among others.

(a)

(b)

(c)

Fig. 8 – Instrumentation applied in building; (a) accelerometers, (b) laser transducers, (c) displacement potentiometers

3.4. Input motion

The specimen was subjected to an artificial record five times. The artificial record with a 1.0 scale factor was representative of the Japanese Building Code design spectra for ordinary buildings. The input record acceleration history and response spectra for a scale factor of 1.0 are shown in Fig. 9. The scale factors adopted for each excitation were as follows:

i) 0.2 (for confirming serviceability performance objectives were satisfied for frequent shaking events);

ii) 1.0 (for confirming that the building could remain mostly elastic with a peak inter-story drift of less than 0.33% at design-level shaking);

iii) 1.5 run #1 (for evaluating the building's performance at 1.5 timed design-level shaking);

iv) 1.5 run #2 (this was repeated to evaluate if the building could withstand an aftershock of equal intensity to its design demand as required by the Japanese Building Code); and

v) 1.6 (for observing the building's performance in its fully inelastic range and its capability to withstanding multiple significant seismic events).

White noise excitations were applied before and after each of the five major excitations. These were used to track changes in the building's dynamic properties resulting from each shaking event.

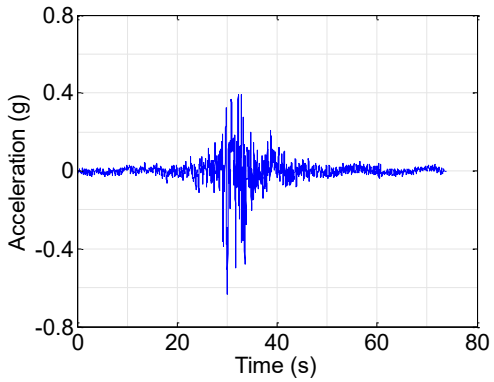

(a)

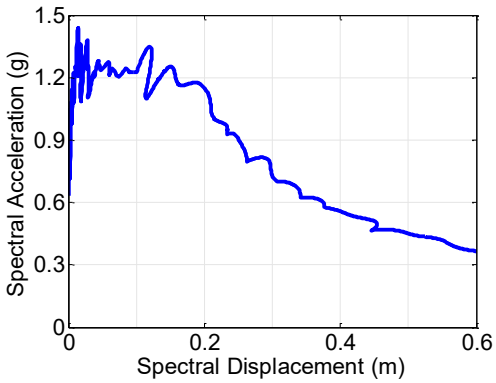

(b)

Fig. 9 – Artificial record with 1.0 scale factor; (a) total acceleration history and (b) response spectra

4. Initial Damage Observations and Evaluations

This section covers initial damage observations and evaluations. No detailed results were discussed as these were still being processed at the time of writing. Building damage surveys were performed (i) before testing, (ii) after the 1.0-scaled excitation, (iii) after the first 1.5-scaled excitation, and (iv) after the 1.6-scaled excitation. After (ii) and (iii), the building damage was evaluated following the "Guideline for Post-Earthquake Damage Evaluation and Rehabilitation of RC Buildings" [10].

Before testing, initial cracks were observed at the beam-wing wall joints adjacent to the outer (C2) columns. These cracks were small (0.2 mm or less in the beams) and were thought to not significantly influence building strength. No damage was observed in columns or slabs.

Following the 1.0-scaled excitation, more cracks were identified at each beam end, though damage was concentrated on a single crack. Minor insignificant cracking had formed on columns and slabs, the latter of which originated near wall gaps and propagated towards the center of the slab. Based on the damage evaluation procedure [10], the damage was minor on 1F and 2F. The damage on 3F was considered moderate if the hanging-wall crack width was considered. However, this occurred where there were no reinforcing and thus had no influence on strength. If the beam residual crack was considered, the 3F damage would be slight.

Following the first 1.5-scaled excitation, only a few new cracks were observed. However, the largest residual beam cracks widened to 2.0 mm. Horizontal cracks with residual width of 0.3 mm formed at column bases and some crushing occurred at wing-wall corners. Slab cracks intersected, resulting in large cracks spanning the slab width residual widths of 3.5 mm. The damage was evaluated as "significant" on all floors.

Photos of final observed damage is shown in Fig. 10. Significant concrete spalling occurred on 1F and 2F beams (Fig. 10a) resulting in reinforcing bars being exposed. While concrete spalling also occurred on 3F (Fig. 10b), the extent was not as significant, and no reinforcing was not exposed. This showed the advantage of the concrete-filled-gap detailing which lessened the compression strains at the soffit of the beam. Significant concrete crushing occurred at the base of the wing-walls (Fig. 10c), and small diagonal column cracks started forming. The slab cracks widened to over 15.0 mm and diagonal cracks formed due to secondary compression struts developing due to a change in the force transfer mechanism. Due to the extensive damage observed, the damage was classified as "significant" and was deemed close to collapse.

(a) (b) (c) (d)

Fig. 10 – Damage observation photos (after 150-1); (a) 2F beam, (b) 3F beam, (c) column base, (d) slab

5. Structural Health Monitoring

Several structural health monitoring approaches were applied to the building to evaluate its performance and safety. One such approach was the use of accelerometer data following Kusunoki [9], and another was using laser scanning and motion tracking technology to capture damage and track building response. Other approaches were also utilized, but only these were described herein.

5.1 Damage evaluation using the Wavelet Transform Method

The approach by Kusunoki [9] involved (i) double integrating accelerometer data to obtain relative displacement response, (ii) simplifying the response into an equivalent single-degree-of-freedom response

using modal analysis methods considering the displaced shape at each time-step, (iii) applying the Wavelet Transform Method and selecting ranks representing the predominant response, and (iv) obtaining the resultant "skeleton curve" from the representative acceleration-displacement response. The skeleton curve obtained from preliminary application of this approach using the experimental data is shown in Fig. 11.

The skeleton curves are useful in several ways. Firstly, the change in the "initial" period could be estimated based on the change of the initial slope with each excitation. Secondly, the overall building ductility demand could be estimated based on the ratio of peak representative displacement to estimated yield displacement. Thirdly, if a "safety limit" is known, one could assess how close the building is to reaching this safety limit, essentially providing an alternative to the damage evaluation procedure [10] followed previously. One important advantage is that this system can be applied in real-time, meaning that the safety of the building could be evaluated almost immediately. This can reduce the time and effort required to evaluate a building's level of safety.

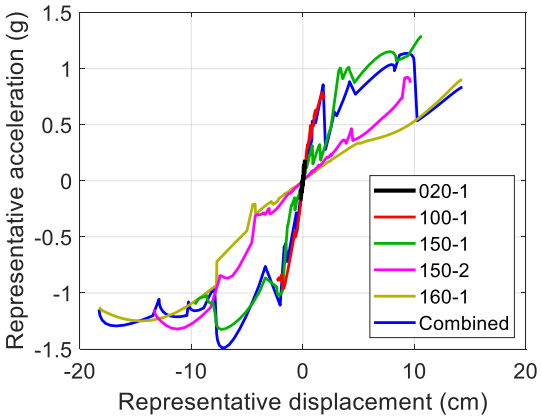

Fig. 11 – Derived capacity curves using WTM

5.2 Laser scanning and motion tracking technology

Two separate research teams were involved with using laser scanning and motion tracking technology; (i) the University of Washington (UW) and University of Nevada, Reno (UNR) team, and (ii) the Building Research Institute (BRI) from Tsukuba, Japan.

The UW/UNR team were funded by the US National Science Foundation (NSF), and collaborated in the project by collecting response and damage data using multiple non-contact image and lidar based systems. UW researchers employed equipment provided by the NSF-funded Natural Hazards Engineering Research Infrastructure (NHERI) "RAPID" Facility. This included two portable lidar scanners, each with integrated imaging but with different lidar scan resolutions and scan times (Leica ScanStation P50 and Leica RTC360), and a surveying total station (Leica Nova TS161). Data collection activities were performed while the structure was stationary (i.e. prior to testing and at the end of each test day) and included:

i) Use of the total station to locate, with a high level of accuracy, approximately 30 high-contrast targets located on the test specimen, the shake table, and the laboratory structure to provide information about residual deformation of the test specimen;

ii) Use of the Leica RTC 360 scanner to generate a modestly accurate/dense 3D point cloud encompassing the interior and exterior of the specimen with image overlay (Fig. 12a) to qualitatively assess the structural performance and support use of localized, high-resolution point cloud data; and,

iii) Use of the Leica P50 to generate high accuracy/density point clouds in regions with significant damage (Fig. 12b) to evaluate the potential for lidar to be used to identify cracks in concrete and masonry structures as well as to determine crack length, width and depth.

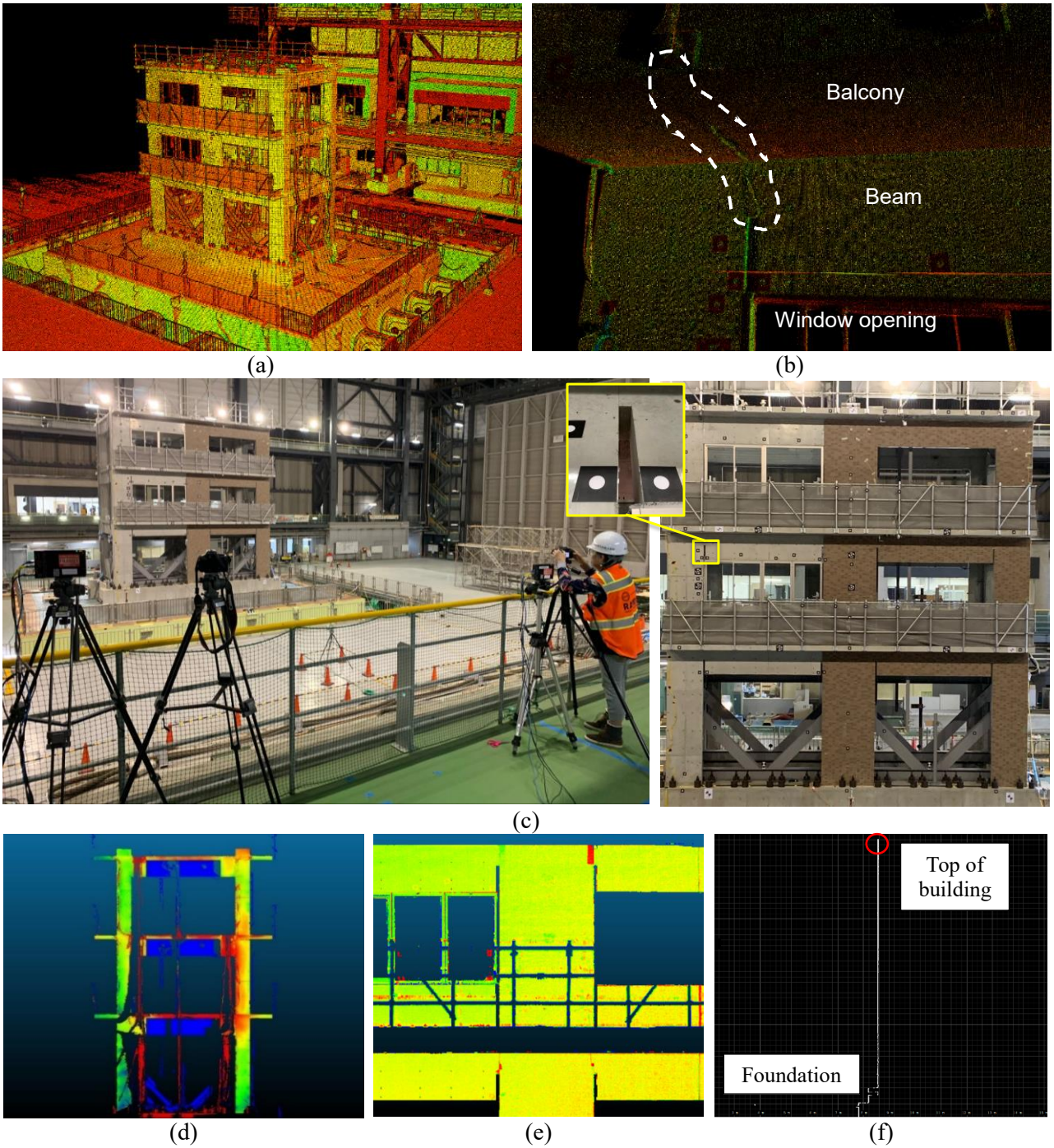

Fig. 12 – Laser scanning and motion tracking examples; (a) point cloud density of specimen, shake table, and laboratory, (b) high-resolution scale of crack initiating from hanging-wall gap, (c) camera setup for TT-DIC monitoring, (d) residual deformation of building, (e) detecting tile damage, and (f) dynamic tracking of specimen response

The UW/UNR team also collected dynamic response data during shake table tests, under both white noise and seismic excitation. The UW team employed the Leica P50 scanner in "line-scan" mode to track the east-west (EW) location of the vertical centerline of the northwest column to generate EW displacement, velocity, and acceleration histories for the column. The UNR team employed two cameras sets; (i) two state-of-the-art monochrome ultra high-speed Fastec cameras and (ii) consumer-grade DSLR Canon cameras (Fig.

12c). These cameras faced the south side of the building on which approximately 40 high-contrast targets were placed as shown in Fig. 12c. Software produced by GOM [11] will be used to perform target-tracking digital image correlation (TT-DIC) of data to generate displacement time-histories for the high-contrast targets. One challenge was dealing with low light levels which were required to avoid potentially interfering with laser sensor readings employed by other research teams. This will require pre-processing of image data to ensure accurate calculation of camera and target locations. Two types of analyses will be conducted using TT-DIC data; (i) determining building frequency and mode shapes using acceleration readings, and (ii) obtaining peak and residual drifts from each excitation. The response and damage data obtained by the UW/UNR team will be compared with similar data collected by other research teams.

The BRI team also conducted similar scans using their own set of equipment. Description of past deployment of such equipment and examples demonstrating the usefulness of acquired data are available in literature [12]. Some initial outputs from their data collection in this project can be seen in Figs. 12d-12f and included (i) evaluating the residual deformation of the building, (ii) identifying exterior damage, such as spalling of tiles, and (iii) tracking the dynamic specimen response.

6. Blind Prediction Competition

In addition to the E-Defense test, a blind prediction competition was held to evaluate the accuracy and reliability of numerical modelling approaches and assumptions. Participants were requested to predict the following building response parameters for the 1.0 and 1.5 (run 1) scaled excitation cases:

i) Roof displacement history (relative to base of building);

ii) Peak absolute interstory drift on all floors; and

iii) Peak base shear demand.

The blind prediction competition was still running at the time of writing, and thus only the judging criteria was discussed here. Contestants will be ranked for each category based on the calculated error, and the three contestants with the best average rank will be deemed competition winners. If a top-three could not be clearly identified due to multiple teams having the same average rank, then the ranking in the roof displacement history category will be used as a tiebreaker as this is thought to be the hardest to predict. The error for roof displacement history were determined using sum-squared-error, SSE_{RDH}, using the following equation.

$$SSE_{RDH} = \sum_{i=1}^{n} \left(x_{predicted,i} - x_{measured,i}\right)^2 \quad (1)$$

Where $x_{predicted,i}$ and $x_{measured,i}$ are the predicted and measured roof-displacements at step i, respectively, and n is the number of steps.

Accuracy of peak values of predicted and measured values ($R_{max,predicted,j}$ and $R_{max,measured,j}$, respectively) were also assessed using sum-square-error considering each floor (denoted by j), though the natural log values were used instead. Base shear was also evaluated using log values, though as only one value was considered for each excitation, the sum-squared-error calculation was not required.

$$SSE_{drift} = \sum_{j=1}^{3} \left(ln\left(R_{max,predicted,j}\right) - ln\left(R_{max,measured,j}\right)\right)^2 \quad (2)$$

7. Conclusions

This paper summarized various aspects of a shake-table test of disaster management center performed at E-Defense in December 2019 and serves as a companion paper to an organized session to be held at the 17th World Conference on Earthquake Engineering. Based on building response and initial damage evaluations,

the building was able to satisfy design objectives from a performance perspective (i.e. minor damage at design-level shaking and ability to survive multiple significant events without collapsing), though the damage at 1.5-times design-level shaking was classified as "significant". Application of various structural health monitoring approaches, such as deriving capacity curves using accelerometer data or using laser scanning and motion tracking technology, demonstrated its effectiveness in rapidly assessing a building's performance and damage.

8. Acknowledgement

The present work is supported by the Tokyo Metropolitan Resilience Project of the National Institute for Earth Science and Disaster Resilience.

Material related to UW/UNR team's contribution presented in this paper is based upon work supported by the US National Science Foundation under awards CMMI-1611820 and CMMI-2000478. Any opinions, findings, and conclusions or recommendations expressed in this material are those of the authors and do not necessarily reflect the views of the National Science Foundation.

Finally, we would also like to acknowledge the many teams and participants involved in the test which enabled it to be a success.

9. References

[1] Hirata N (2017): Introduction to the Tokyo Metropolitan Resilience Project, *NHERI-NIED Plenary Session Presentation* [powerpoint presentation].

[2] Cooper M, Carter R, Fenwick R (2012): Final Report Volume 6 – Canterbury Television Building (CTV). Canterbury Earthquake Royal Commission, New Zealand.

[3] Matsuda T, Yamao T, Matsuda H, Kakimoto R, Tsujimoto G, Kasai A, Fujimi T, Maruyama T, Yoshito K, Torii M, Inamoto Y, Yukihide K, Tamai H, Choi J, Yamazaki T, Yoshida M (2016): 2016 Kumamoto earthquake emergency disaster report – part 2 (in Japanese). The Japan Society of Civil Engineers (west chapter).

[4] Nishiyama I, Okawa I, Fukuyama H, Okuda Y (): Building damage by the 2011 off the Pacific coast of Tohoku earthquake and coping activities by NILIM and BRI collaborated with the administration. *43rd Joint Meeting of U.S.-Japan Panel on Wind and Seismic Effects*, Tsukuba, Japan.

[5] Ministry of Land, Infrastructure, Transport and Tourism (2018): Design guideline for buildings with post-disaster functions (draft)". *Technical Note of National Institute for Land and Infrastructure management*, No. 1004.

[6] Kono S, Kitamura F, Yuniarsyia E, Watanabe H, Mukai T, Mukai DJ (2017): Efforts to Develop Resilient Reinforced Concrete Building Structures in Japan. *Fourth Conference on Smart Monitoring, Assessment and Rehabilitation of Civil Structures*, Zurich, Switzerland.

[7] Tani M, Mukai T, Demizu T, Kono S, Kinugasa H, Maeda M (2017): Full-scale Static Loading Test on a Five Story Reinforced Concrete Building (part 2: damage analysis). *16th World Conference on Earthquake Engineering*, Santiago, Chile.

[8] Fukai S, Kusunoki K, Yeow TZ (2019): A new safety evaluation system and the continuous functionality of buildings with post-disaster functions following earthquakes (part 1 – design of specimen). *2019 Annual Meeting of the Architectural Institute of Japan*, Kanazawa, Japan.

[9] Kusunoki K, Hinata D, Hattori Y, Tasai A (2018): A New Method for Evaluating the Real-Time Residual Seismic Capacity of Existing Structures using Accelerometers: Structures with Multiple Degrees of Freedom. *Japan Architectural Review*, **1**(1), pp 77-86.

[10] Maeda M, Kang DE (2009): Post-earthquake damage evaluation of reinforced concrete buildings. *Journal of Advanced Concrete Technology*, **7**(3), 327-335.

[11] GOM (2011): GOM 3D Software [online]. Braunschweig, Germany. https://www.gom.com/3d-software.html (date accessed: 27th January 2020)

[12] Mukai T, Watanabe H, Sakota T, Kaneko O, Narita S, Kubo K, Kudo R, Kakizaki K, Takahashi G (2018): Damage investigation for structural members of superstructure in damaged local government office building due to the 2016 Kumamoto Earthquake. *The 15th Japan Earthquake Engineering Symposium*, Sendai, Japan.

